Bioconjugate Chemistry

Article

pubs.acs.org/bc

Generation and Characterization of Virus-Enhancing Peptide Nanofibrils Functionalized with Fluorescent Labels

Sascha Rode,[†] Manuel Hayn,[†] Annika Röcker,[†] Stefanie Sieste,[‡,⊥] Markus Lamla,[‡,⊥] Daniel Markx,[#] Christoph Meier,[‡] Frank Kirchhoff,[†,∥] Paul Walther,[§] Marcus Fändrich,[#] Tanja Weil,[‡,⊥,∥] and Jan Münch*[,†,∥,▽]

[†]Institute of Molecular Virology, Ulm University Medical Center, Meyerhofstraße 1, 89081 Ulm, Germany

[‡]Institute for Organic Chemistry III, [§]Central Facility for Electron Microscopy, and [∥]Ulm-Peptide Pharmaceuticals, Ulm University, Albert-Einstein-Allee 11, 89081 Ulm, Germany

[⊥]Max Planck Institute for Polymer Research, Ackermannweg 10, 55128 Mainz, Germany

[#]Institute of Protein Biochemistry, Ulm University, Helmholtzstraße 8/1, 89081 Ulm, Germany

[▽]Core Facility Functional Peptidomics, Ulm University Medical Center, Albert-Einstein-Allee 11, 89081 Ulm, Germany

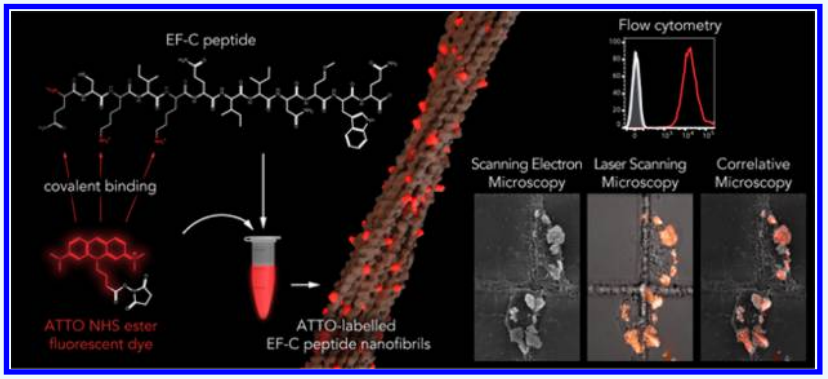

ABSTRACT: Retroviral gene transfer is the method of choice for the stable introduction of genetic material into the cellular genome. However, efficient gene transfer is often limited by low transduction rates of the viral vectors. We have recently described a 12-mer peptide, termed EF-C, that forms amyloid-like peptide nanofibrils (PNF), strongly increasing viral transduction efficiencies. These nanofibrils are polycationic and bind negatively charged membranes of virions and cells, thereby overcoming charge repulsions and resulting in increased rates of virion attachment and gene transfer. EF-C PNF enhance vector transduction more efficiently than other soluble additives and offer prospects for clinical applications. However, while the transduction-enhancing activity of PNF has been well-characterized, the exact mechanism and the kinetics underlying infection enhancement as well as the cellular fate of the fibrils are hardly explored. This is partially due to the fact that current labeling techniques for PNF rely on amyloid probes that cause high background staining or lose signal intensities after cellular uptake. Here, we sought to generate EF-C PNF covalently coupled with fluorescent labels. To achieve such covalent bioconjugates, the free amino groups of the EF-C peptide were coupled to the ATTO 495 or 647N NHS ester dyes. When small amounts of the labeled peptides were mixed with a 100- to 10 000-fold excess of the native peptide, PNF formed that were morphologically indistinguishable from those derived from the unlabeled peptide. The fluorescence of the fibrils could be readily detected using fluorescence spectroscopy, microscopy, and flow cytometry. In addition, labeled and nonlabeled fibrils captured viral particles and increased retroviral transduction with similar efficacy. These covalently fluorescence-labeled PNF are valuable tools with which to elucidate the mechanism(s) underlying transduction attachment and the fate of the fibrils in cells, tissues, and animal models.

INTRODUCTION

Low transduction efficiencies are a major drawback of retroviral gene transfer.[1,2] The main reason for inefficient transduction rates is the electrostatic repulsion between the negatively charged viral and cellular membranes.[3,4] Several additives based on soluble cationic polymers, such as hexadimethrine bromide (Polybrene) and diethylaminoethyl (DEAD)-dextran, have been used for decades to increase the rates of viral attachment to the cell surface and hence viral entry into the cell.[5,6] However, most polycations are cytotoxic and not very efficient.[7−11] We and others have recently described peptide nanofibrils (PNF) as a novel, highly efficient, and safe class of retroviral transduction enhancers.[12−17] PNF form by self-assembly of peptides into well-ordered fibrillar structures that share biochemical and biophysical

Received: February 14, 2017
Revised: March 10, 2017
Published: March 16, 2017

DOI: 10.1021/acs.bioconjchem.7b00079
Bioconjugate Chem. 2017, 28, 1260−1270

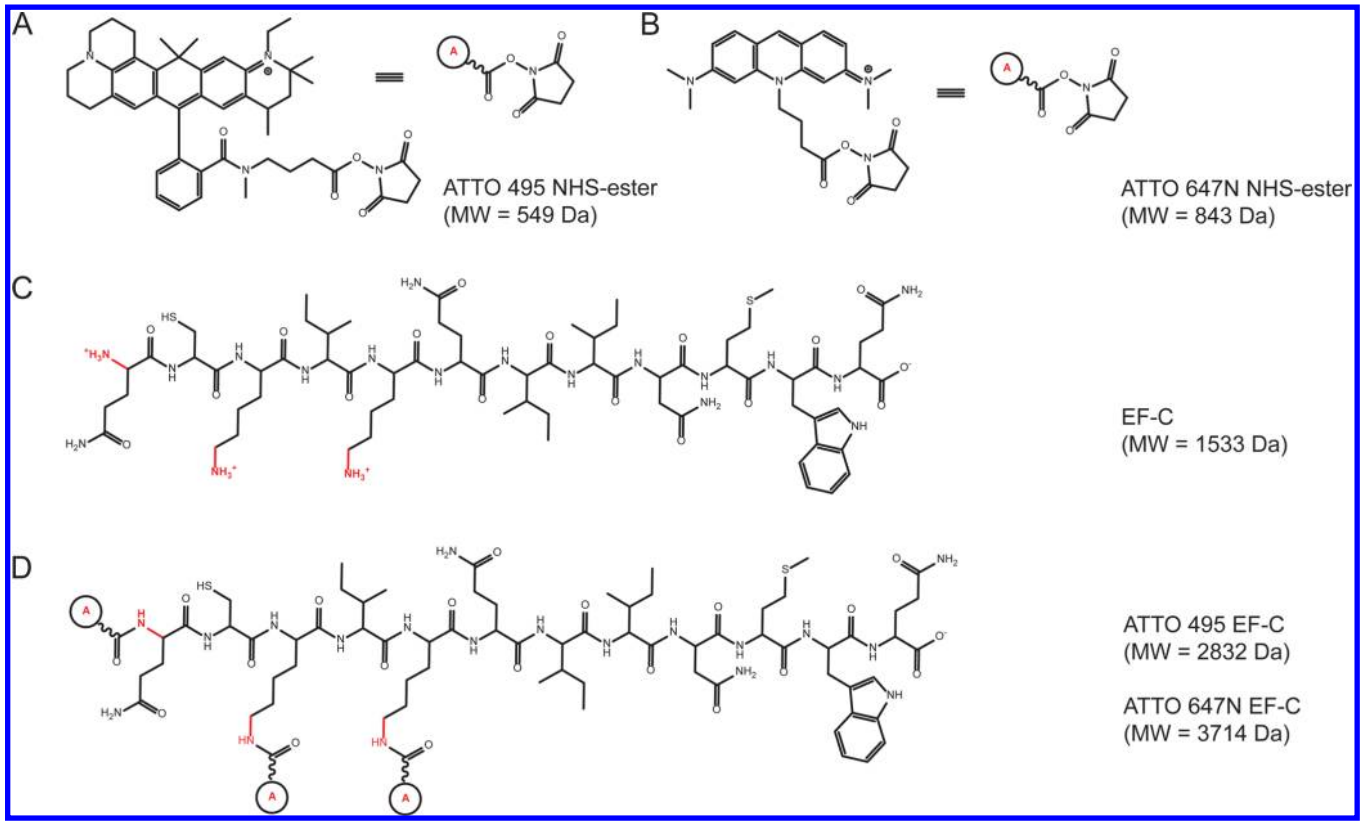

Figure 1. Chemical structure of ATTO dyes and EF-C peptide. (A) Structure of ATTO 495 NHS ester. (B) Structure of ATTO 647N NHS ester. (C) Structure of EF-C monomeric peptide.[13] Primary reactive amino groups are marked in red. (D) Structure of the ATTO EF-C peptide. The three potential free amino groups at neutral pH were labeled with NHS ester.

properties with amyloid fibrils: they exhibit green birefringence after staining by the amyloid dye Congo red, show shifts in their fluorescence spectrum upon binding to thioflavin T (ThT), exhibit characteristic patterns by X-ray diffraction, feature β-sheet-rich secondary structures as indicated in Fourier transform infrared (FTIR) spectra, and form fibrillar structures visible by transmission electron microscopy (TEM).[18,19]

The best-characterized and most potent PNF-based transduction enhancer is derived from an amphiphilic 12-mer peptide derived from the HIV glycoprotein gp120, termed enhancing factor C (EF-C).[13] This peptide with the sequence QCKIKQIINMWQ_ instantaneously forms fibrils when dissolved in polar solvents.[13] The fibrils are hundreds of nanometers long and have diameters of ∼3 nm.[13] Like other transduction enhancers, EF-C PNF display positive ζ potentials at neutral pH and are thus polycationic. Transduction enhancement is mediated through electrostatic interactions between the positively charged fibrils and negatively charged viral and cellular membranes.[12,13,20−22] This overcomes the charge repulsions of the membranes and results in increased rates of virion attachment and fusion with target cells. This mechanism is supported by data showing that abrogating the cationic properties of the fibrils through anionic polymers diminishes their ability to enhance infection.[20−23] Of note is the fact that EF-C PNF are not cytotoxic at concentrations allowing maximal transduction enhancement and do not alter the differentiation capacity of human hematopoietic stem cells.[13] EF-C PNF increase retroviral transduction more efficiently than other commercially available additives and have now been commercialized under the brand name Protransduzin.[12,13,24] Thus, PNF represent a highly versatile, effective, and broadly applicable nanomaterial that might significantly facilitate viral gene transfer in basic and clinical research applications.

We have shown that EF-C PNF bind to the surface of cells. It is currently unclear, however, whether the fibrils remain at the surface or get internalized and degraded, stored, or eventually released.[13] Studying the dynamics of the interaction of PNF with cells and intracellular transport requires labeling of the fibrils, preferentially with fluorescent probes, allowing the tracking of the fibrils by fluorescence microscopy and other techniques over extended time periods. Various labeling methods for amyloid fibrils have been described.[25−27] Probably the most widely used technique involves staining with Congo red, a secondary diazo dye showing yellow-green birefringence under crossed polarized light.[25−27] Another commonly used dye is ThT, a benzothiazole salt that presumably intercalates into the β-sheet structure of amyloid fibrils to induce a characteristic red shift in its fluorescence emission spectrum.[28−30] Although ThT allows convenient and well-affordable detection of amyloid in reaction tubes, its application in complex environments such as cells or tissues is limited due to high background signals.[25,31,32] A novel derivative of ThT that yields a brighter signal over a wider dynamic range is ProteoStat.[31] Both ThT and ProteoStat are molecular rotor dyes that noncovalently and selectively interact with aggregated protein to alter fluorescence signals.[31] Other newly developed sensitive fluorescent amyloid probes are luminescent conjugated oligothiophenes, e.g., the pentameric thiophene derivative p-FTAA.[31,33] All of the above-mentioned amyloid probes allow the detection and quantification of EF-C PNF.[13,34] However, they generally come with the caveat of causing high background activities in protein rich body fluids, cells, or tissues.[22,31,34−36]

DOI: 10.1021/acs.bioconjchem.7b00079
Bioconjugate Chem. 2017, 28, 1260−1270

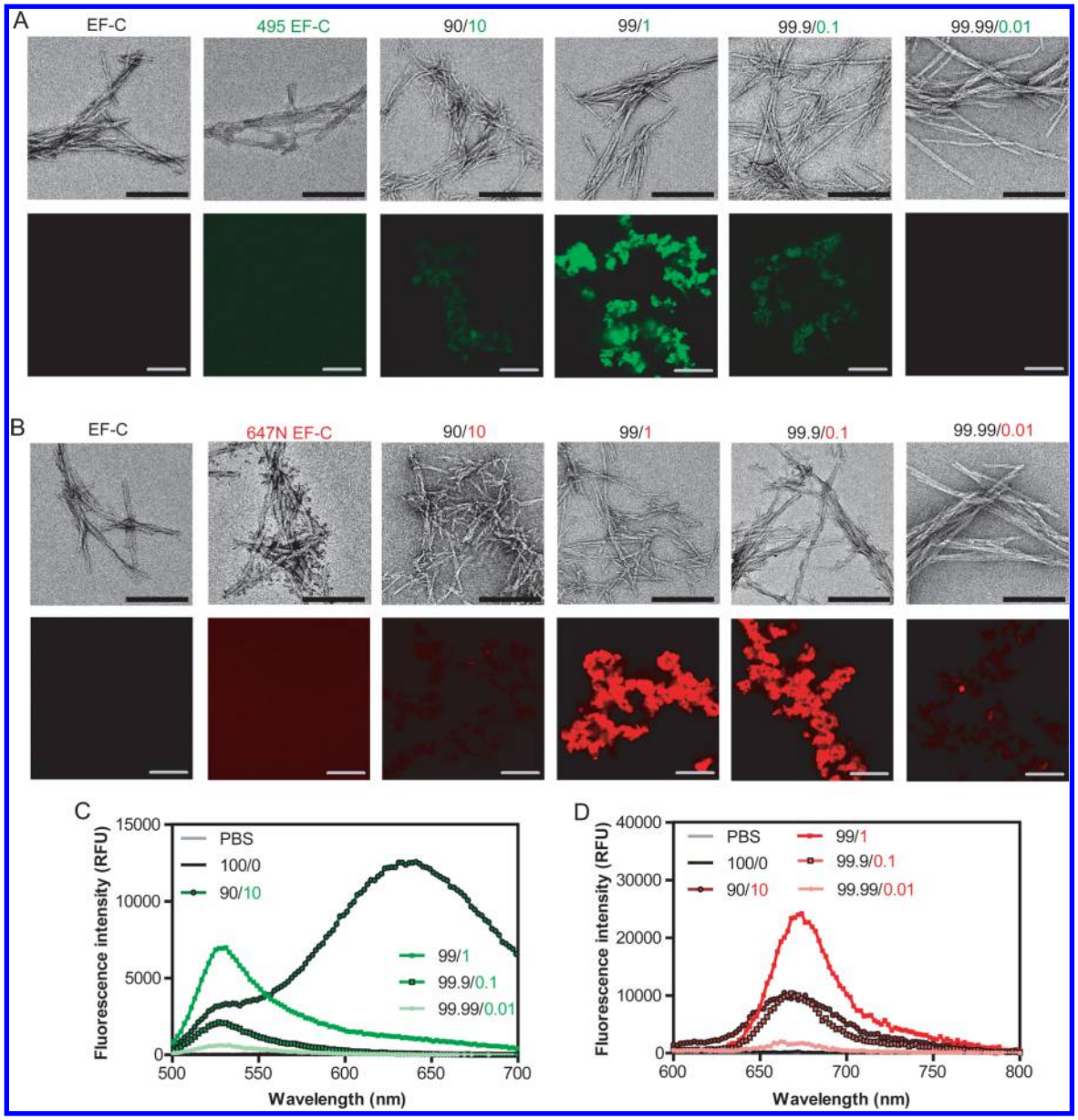

Figure 2. Morphology and fluorescent properties of generated fibrils. (A) Electron micrographs (upper panel; scale: 200 nm) and confocal images (lower panel; scale: 10 μm) of newly generated ATTO 495−EF-C fibrils. EF-C represents the unlabeled peptide only, and 495 EF-C represents the labeled peptide only. (B) Electron micrographs (upper panel; scale: 200 nm) and confocal images (lower panel; scale: 10 μm) of newly generated ATTO 647N−EF-C fibrils. EF-C represents the unlabeled peptide only, and 647N−EF-C represents the labeled peptide only. (C) Fluorescence spectra of ATTO 495−EF-C fibrils with a maximum at 531 nm (excitation: 465 nm). (D) Fluorescence spectra of ATTO 647N−EF-C fibrils with a maximum at 674 nm (excitation: 547 nm). RFU, relative fluorescence units.

We believe that this limitation is due to the noncovalent binding of the probes, which is a dynamic process leading to loss of signal and reduced specificity in complex mixtures, e.g., under in vivo conditions and extended observation times.[37−39] Moreover, the fluorescence emission spectra of these amyloid probes are not tunable, which restricts applications such as multicolor flow cytometry or confocal microscopy.

To overcome these limitations, we here generated EF-C PNF that were covalently linked with fluorescent labels. These fluorescent PNF are structurally similar to parenteral EF-C PNF and allow detection using fluorescence-based techniques. Importantly, the covalently labeled EF-C PNF are not cytotoxic and enhance retroviral infection as efficiently as nonlabeled fibrils. We show that labeled fibrils are more stable than EF-C PNF stained with noncovalent probes and allow a significantly more-sensitive detection of fibrils in cell culture. We believe that covalently labeled EF-C PNF represent a powerful tools to study the interaction of fibrils with cells with high contrast and stability and therefore outperform current labeling approaches. Our results will have a great future impact for studies aiming to analyze the interaction of amyloid fibrils with cellular surfaces, along with their internalization, storage, or degradation. Moreover, the stable fluorescent label should now also allow us to study the biodistribution and stability of functionally active PNF in animal models.

RESULTS

Generation of ATTO 647N- and 495-Labeled EF-C PNF. We have chosen the fluorescent ATTO 495 (Figure 1A)

DOI: 10.1021/acs.bioconjchem.7b00079
Bioconjugate Chem. 2017, 28, 1260−1270

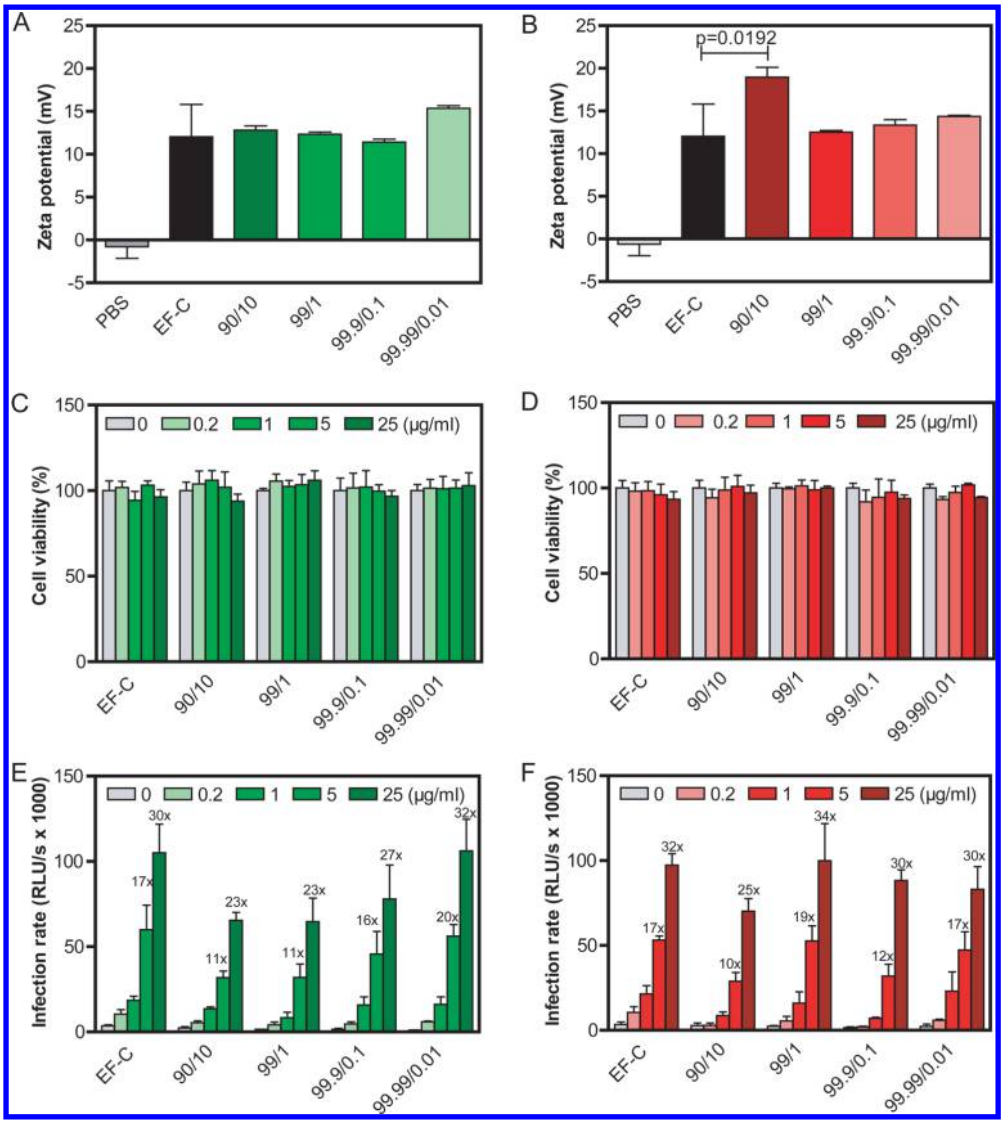

Figure 3. HIV-enhancing activity of covalently labeled fibrils. (A and B) ζ potentials of (A) ATTO 495- and (B) 647N-labeled EF-C PNF. (C) ATTO 495- and (D) 647N-labeled EF-C PNF do not affect viability of TZM-bl cells at concentrations up to 25 μg/mL on TZM-bl cells. (E) ATTO 495- and (F) 647N-labeled EF-C PNF enhance viral infection rates of HIV-1. Viral particles were incubated with the indicated concentrations of fibrils and then used to inoculate TZM-bl cells, resulting in a 10-fold dilution of PNF. Infection rates were determined 3 days later by quantifying ß-galactosidase activity in cellular lysates by a luminescence assay (relative light units per second, RLU/s). Numbers above columns indicate the *n*-fold infection enhancement relative to PBS-exposed virus. All values shown are mean values derived from three technical (panels A and B) or biological (panels C–F) replicates ± standard deviation.

and 647N (Figure 1B) labels as they exhibit a green and red fluorescence, respectively, which are detectable by most flow cytometers. Both labels are characterized by strong absorption, high fluorescence quantum yields, and high thermal stability and photostability as well as a high stability toward atmospheric ozone, which makes them ideally suited for fluorescence-based microscopy studies. Moreover, ATTO 647N absorption and fluorescence properties are stable in a pH range between 2 to 11, and they should thus not be affected by the acidic environment existing, e.g., in cellular lysosomes.[42] To generate chromophore labeled EF-C (1533 Da), a 2-fold molar excess of *N*-hydroxysuccinimide esters of ATTO 495 (549 Da) or ATTO 647N (843 Da) were added to an EF-C peptide in DMSO, as described in the Experimental section. The mixture was incubated and processed following the manufacturer's instruction, yielding covalent conjugates in which the respected chromophore is attached to maximum of three potential free amino groups of the peptide (Figure 1C). The resulting ATTO 495- or 647N-labeled EF-C peptides have molecular weights of 2832 and 3714 Da, respectively if all three binding sites are labeled (Figure 1 D). However, it is notable that no labeling or single- or double-labeling of the monomeric peptide can occur, as verified by matrix-assisted laser desorption–ionization (MALDI) measurement.

To evaluate whether the covalently labeled peptides form fluorescent nanofibrils, they were diluted in PBS to induce self-assembly.[13] Unlabeled EF-C was used as control. Thereafter, the solutions were analyzed by transmission electron microscopy (TEM). The parenteral noncoupled peptide formed a mesh of aggregated fibrils (Figure 2A,B, upper panels). The ATTO 495- and 647N-labeled EF-C solutions also formed fibrils but to a significantly lesser extent (Figures 2A,B; data not shown). The fluorescence of the fibrils was then studied at excitation at 488 nm for (ATTO 495) or 633 nm (ATTO

DOI: 10.1021/acs.bioconjchem.7b00079
Bioconjugate Chem. 2017, 28, 1260–1270

647N) using confocal imaging. As expected, PNF derived from parenteral EF-C peptide showed no fluorescence (Figure 2A,B; bottom panels). Less predictively, PNF derived from ATTO 495- or ATTO 647N-labeled peptides only produced a diffuse fluorescence signal (Figure 2A,B). This is likely due to intra- or intermolecular quenching effects that may occur through quenching due to strongly interacting chromophores leading to a shortening of the fluorescence lifetime and reduced fluorescence intensities.[43−45]

We next sought to generate fluorescent PNF by mixing DMSO stocks of unlabeled and labeled EF-C peptides. Specifically, 90/10, 99/1, 99.9/0.1 and 99.99/0.01 ratios of unlabeled versus labeled peptides in DMSO were mixed and subsequently diluted in PBS to induce fibril formation. TEM analyses demonstrated that all samples containing a 10-fold and higher excess of unlabeled peptide formed fibrillary structures that were structurally similar to parenteral EF-C-based PNF (Figure 2A,B). Fluorescence microscopy revealed that fibrils formed by peptide mixtures containing a 100-fold (99/1) or 1000-fold (99.9/0.1) excess of unlabeled peptide were readily detectable as "green" (Figure 2A, Ex_{max} = 526 nm) or "red" (Figure 2B, Ex_{max} = 559 nm) fluorescent nanostructures that closely resembled those of EF-C derived PNF stained with the amyloid probe ProteoStat.[13] Fibrils generated from mixtures containing a 10 000-fold (99.99/0.01) excess of unlabeled peptide only produced a faint fluorescent signal (Figure 2A,B), which became undetectable when the amounts of labeled peptides was further decreased (data not shown).

We next determined the emission spectra of the generated EF-C fibrils by excitation at 465 nm (for ATTO 495) and 547 nm (for ATTO 647N), respectively. The parenteral EF-C PNF and the buffer control (PBS) did not result in a detectable signal (Figure 2C,D) indicating that nonspecific background emission is low. However, fluorescence intensities increased and peaked for ATTO 495-containing fibrils at 531 nm (Figure 2C) and ATTO 647N at 674 nm (Figure 2D) in all samples containing the labeled peptides. Samples containing 1% labeled peptide (99/1) resulted in highest fluorescence intensities (Figure 2C,D). In the sample containing 10% ATTO 495-labeled peptide, a second peak at around 640 nm was detectable, which is likely due aggregation of highly lipophilic ATTO 495 chromophores, as communicated by the manufacturer. Taken together, these findings demonstrate that EF-C-based fluorescent PNF were generated at optimum chromophore-to-peptide ratios, and the resulting fibrils structurally resembled those of the parenteral EF-C PNF.

Covalently Labeled ATTO 495 and 647N EF-C PNF Have Cationic Properties and Boost Retroviral Transduction Properties. The positive net surface charge of PNF is important for viral transduction enhancement.[12,13,20,21] We found that all fluorescent EF-C PNF display positive ζ potentials, similar to the parenteral PNF (Figure 3A,B). The ζ potential of the 90/10 sample was slightly enhanced for ATTO 647N fibrils (Figure 3B), which is likely due to the cationic nature of the dye that carries a net electrical charge of +1.

To determine possible cytotoxic effects of the generated PNF, we performed cell viability assays. For this, TZM-bl cells, a HeLa cell derivate that is widely used to study retroviral infection,[46] were incubated with serial dilutions of the various labeled or unlabeled EF-C-based PNF for 3 days. The metabolic activity of the cells was evaluated by measuring intracellular ATP levels and demonstrated that none of the tested fibrils were cytotoxic at concentrations up to 25 μg/mL (Figure 3C,D).

To clarify whether the fluorescent EF-C PNF enhance retroviral infection, HIV-1 particles that represent prototype retroviral vectors were exposed to the fibrils, and these mixtures were subsequently used to transduce TZM-bl cells. Upon successful infection with HIV-1, the viral Tat protein is expressed and transactivates expression of TZM-bl cell encoded ß-galactosidase, which can be quantified in a luminescence-based assay. As shown in Figure 3E,F, all analyzed samples enhanced viral infectivity with similar activity as the parenteral peptide. For example, exposure of virus to 25 μg/mL of the fibrils (resulting in final cell culture concentrations of 2.5 μg/mL) exhibiting the highest "green" fluorescent intensity (99/1; see Figure 2A) increased infection by 23-fold as compared to the control containing no fibril (Figure 3E). Likewise, the two PNF with highest "red" fluorescence (99/1 and 99.9/0.01) boosted viral infection 34- and 30-fold, respectively (Figure 3F). Thus, fluorescent ATTO 495- and 647N-labeled EF-C PNF display cationic surface charges; they are obviously not cytotoxic, and they are functionally active as they boost retroviral infection as efficiently as the wildtype EF-C PNF.

Long-Lasting Fluorescence of Covalently Labeled EF-C PNF. In principle, covalently labeled PNF should outperform commonly used fibrils stained with p-FTAA, ProteoStat, or ThT that only form supramolecular complexes by exerting a longer-lasting, detectable fluorescence signal. To test this, 100 μg/mL of EF-C PNF that were stained either with the three amyloid probes or coupled with 647N (99/1 ratio) were agitated in PBS, and fluorescence intensities were recorded over 250 min. Already within 25 to 60 min, fibrils stained with ThT and the closely related ProteoStat dye lost ~50% of fluorescence intensities (Figure 4). The fluorescence of p-FTAA-labeled EF-C PNF gradually decreased over time with a half-maximal reduction of the relative fluorescence at ~160 min. In contrast, the fluorescence signal of the ATTO 647N-labeled EF-C PNF remained constantly high throughout the entire observation period (Figure 4).

Sensitive Detection of ATTO 647N-Coupled EF-C PNF in Cell Culture. Next, we compared the sensitivity of detection of covalently and noncovalently labeled fibrils in cell culture

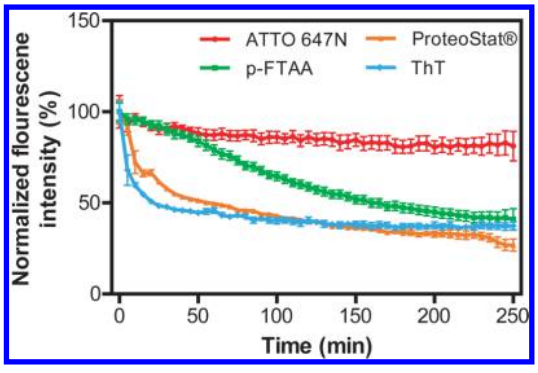

Figure 4. Stability of the fluorescence signal of EF-C PNF over time. ATTO 647N EF-C fibrils 99/1 and amyloid-specific dyes stained fibrils were incubated in PBS, and fluorescent fluorescence spectroscopy was performed every 5 min with 5 s of shaking before each measurement. The following settings were used for ATTO 647N-, p-FTAA-, ProteoStat-, and ThT-labeled fibrils (excitation/emission): 644/669, 450/510, 550/610, and 450/482 nm, respectively. Error bars

DOI: 10.1021/acs.bioconjchem.7b00079
Bioconjugate Chem. 2017, 28, 1260−1270

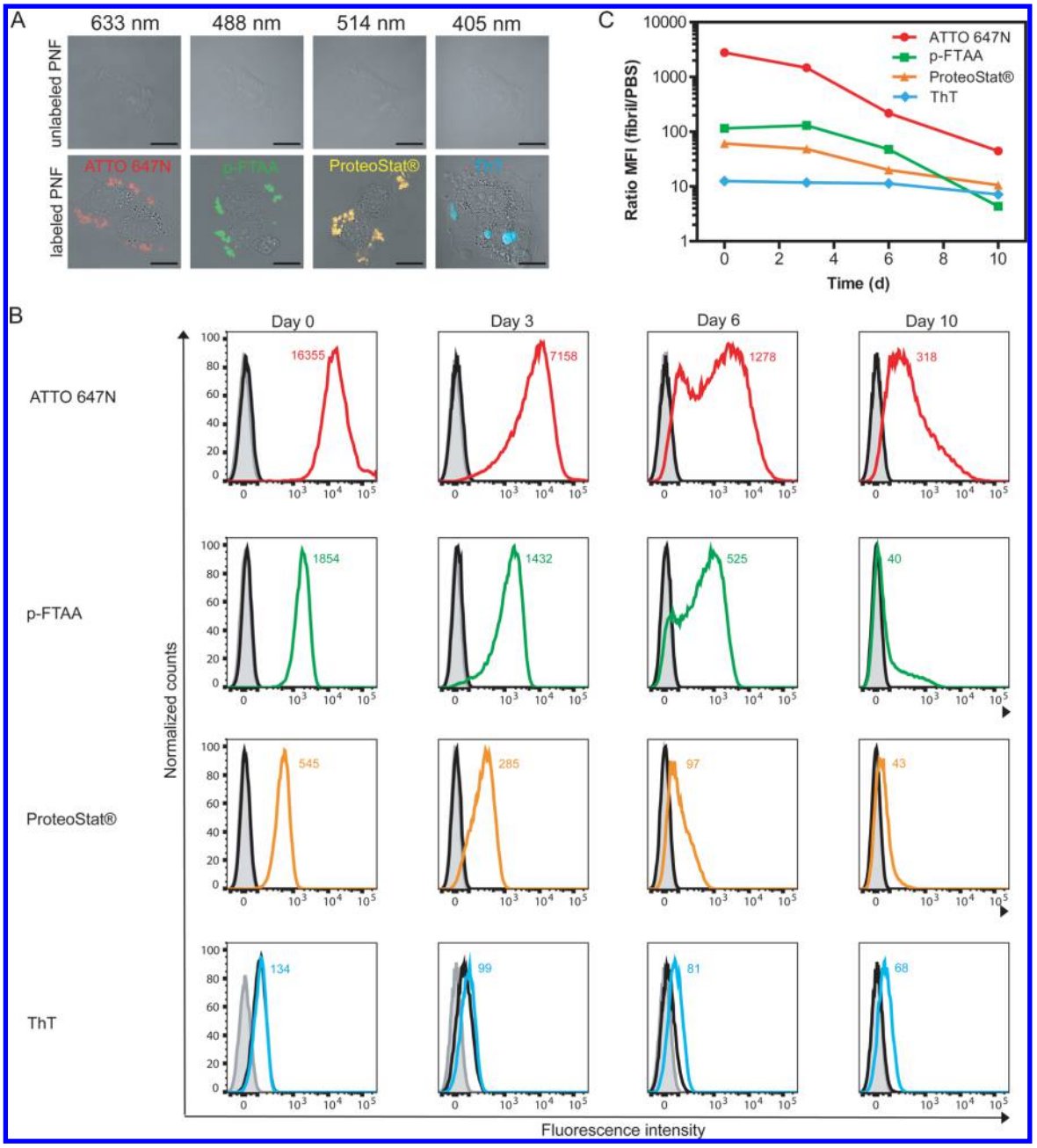

Figure 5. Detection of fluorescent EF-C PNF in cell culture. (A) Laser scanning microscopy of TZM-bl cells incubated for 4 h with 5 μg/mL of the unlabeled or labeled EF-C PNF. Unlabeled EF-C fibrils were not detectable with the applied settings (scale: 10 μm). The following excitation lasers were used for ATTO 647N, p-FTAA, ProteoStat, and ThT: 633, 488, 514, and 405 nm. (B) Flow cytometry analysis of TZM-bl cells that were exposed to 5 μg/mL of the labeled fibrils. Cells were trypsinized and analyzed at indicated time points. The gray line represents the PBS control, the black line represents unlabeled EF-C PNF, and colored lines represent labeled fibrils. The following excitation lasers were used for ATTO 647N, p-FTAA, ProteoStat, and ThT: 640, 488, 488, and 405 nm. The mean fluorescence intensity (MFI) of labeled fibrils is depicted in each panel. (C) Assay sensitivity was calculated by dividing MFI obtained from cells incubated with labeled fibrils through MFI of cells exposed to buffer (see panel B).

using confocal microscopy and flow cytometry. TZM-bl cells were exposed for 4 h to 5 μg/mL of 647N (99/1), p-FTAA, ProteoStat- and ThT-stained PNF, or unlabeled EF-C PNF as control. Thereafter, medium was changed, and cells were fixed and analyzed. As shown in Figure 5A, all labeled PNF were detectable at the cellular surface (Figure 5A, bottom panel), whereas no signal was obtained unlabeled fibrils (Figure 5A, upper panel). These data show that 647N-labeled fibrils interact with the cellular surface, a prerequisite for viral infection enhancement.[12,13,20]

Next, we quantified fluorescence intensities of TZM-bl cells exposed to the differently labeled PNF (5 μg/mL) by flow cytometry over several days. At day 0 (i.e., 4 h post-incubation), cells supplemented with 647N-labeled PNF (99/1) showed the highest mean fluorescence intensity (MFI), with 16 355 arbitrary units that outperformed p-FTAA (MFI: 1854) and ProteoStat (MFI: 545) (Figure 5B). In contrast, ThT-stained PNF were hardly detectable (MFI: 134). The MFI of all samples decreased over time. Signal intensities were close to background for ThT- and ProteoStat-labeled PNF at day 6 and

DOI: 10.1021/acs.bioconjchem.7b00079
Bioconjugate Chem. 2017, 28, 1260−1270

for p-FTAA-stained fibrils at day 10. In contrast, 647N-labeled EF-C PNF were still detectable even after 10 days of incubation (Figure 5B), suggesting that covalently labeled fibrils are also more stable in the presence of cells.

Finally, we determined the sensitivity of detection of the various fluorescent fibrils and calculated the signal-to-noise (S-to-N) ratios by dividing the MFI of cells incubated with labeled PNF through MFI of cells exposed to buffer. The highest ratios were obtained for 647-N-labeled EF-C PNF with S-to-N ratios of 2781 at day 0 and 1472 at day 3, which decreased to a still detectable ratio of 44 at day 10. These values were more than 1 order of magnitude higher than those obtained for p-FTAA-labeled PNF. Lowest S-to-N values were obtained for the commonly used ThT- and ProteoStat-stained PNF. Taken together, these results show that covalently coupled ATTO 647N EF-C PNF are stable in vitro and in vivo and allow a highly sensitive detection of the fibrils in cell culture over extended detection periods.

DISCUSSION

We here describe the generation and functional characterization of EF-C-based PNF covalently linked to fluorescent dyes of the red and green spectral region. These fibrils were generated from the native EF-C peptide labeled at its free amino groups with *N*-hydroxysuccinimid (NHS) activated fluorescent dyes. The EF-C structure is composed of three amino groups (Figure 1C), which are able to undergo nucleophilic reactions with the activated carboxylic acid groups of the NHS esters leading to the desired covalently labeled peptide.[47]

Formation of EF-C PNF is usually initiated by dissolving the peptide DMSO stock solution in polar solvents such as water, PBS, or cell culture medium.[13] However, when pure covalently labeled EF-C peptide was treated the same way, only sparse amounts of nonfluorescent fibrils formed (Figure 2A,B; data not shown). This may be due to steric hindrance as the dye molecule structures are composed of conjugated aromatic rings and thus demand space that might be required for effective aggregation or aggregation of high densities of lipophilic chromophores compete with structured formation of nanofibrils.[48−50] The absence of a defined fluorescence signal is probably due to static self-quenching, a phenomenon that has been described for molecules labeled with multiple copies of the same fluorophore and may originate from identical fluorophores being in strong coupling conditions, i.e., parallel orientation and close proximity to each other.[43,51] Mixing DMSO stocks of labeled and nonlabeled EF-C peptide in ratios of 90/10 to 99.99/0.01 followed by dilution in PBS, however, resulted in the formation of fluorescent fibrils that were morphologically similar to those derived from the parenteral peptide (Figure 2). The broadest fluorescence signal was derived from 99/1 mixtures in the case of the ATTO 495 fibrils and 99/1 and 99.9/0.1 mixtures for the ATTO 647N fibrils. According to the manufacturer, the fluorescence quantum yield of ATTO 495 is around 70% less than for ATTO 647N, ($\eta_{fl(ATTO\ 495)}$ = 20% and $\eta_{fl(ATTO\ 647N)}$ = 65%). We also detected this difference for the labeled peptide fibrils (Figure 2). Our results also imply that the labeled peptide was incorporated into the growing fibril and that high overall fluorescence quantum yields were retained after assembly. It is noteworthy that the covalently labeled EF-C PNF resembled the parenteral EF-C PNF, both structurally and functionally, as they increased retroviral infection with similar efficiencies (Figure 3).

Fluorophore NHS ester coupling has previously been applied to label preformed fibrils.[52−58] We have similarly tried to couple mature EF-C PNF with ATTO 647N but failed to generate fluorescent fibrils with potent virus-enhancing activity (data not shown). An alternative strategy to generate fluorophore-labeled amyloids is to mix labeled with unlabeled polypeptides before fibrillation is initiated, as was done to produce fluorescent α-synuclein or light-chain amyloids.[48,59,60] Likewise, Jin et al. successfully generated ATTO565-coupled Aß(1−42) fibrils through incubating a mix containing 10% labeled and 90% unlabeled peptide.[61] Interestingly, this approach also worked with the EF-C peptide that forms fibrils on a seconds time scale, whereas self-assembly of other amyloids takes days to weeks.

For further analysis, we focused on ATTO 647N-labeled fibrils as they exhibited a higher fluorescence quantum yield than fibrils derived from the ATTO 495-coupled peptide (Figure 2A,B). One main advantage of the covalently labeled fibrils is the long-lasting stability of the fluorescence signal (Figure 4). This is in contrast to the fluorescence intensities of EF-C PNF that were not stained covalently with molecular rotor dyes (ThT or ProteoStat) or p-FTAA that lost signal intensity already during incubation (Figure 4). We also demonstrate that covalently labeled EF-C PNF interact with cellular surfaces, similar to PNF stained with ThT, ProteoStat, or p-FTAA (Figure 5A,B). However, even under these conditions, the covalently labeled fibrils produced a brighter (absolute fluorescence intensity) and more-specific (signal-to-noise ratio) signal in cell culture as compared to noncovalently stained fibrils (Figure 5B,C). Thus, the new covalently labeled EF-C PNF are not only functionally active and enhance viral infection but also can be detected by fluorescence-based techniques with sensitivities exceeding those of other amyloid probes. Interestingly, the fluorescence signal remained detectable in cell culture throughout an observation time of 10 days, which is in contrast to data obtained with ThT or p-FTAA-labeled fibrils. This may be due to the higher stability or the increased fluorescence yield of the ATTO 647N-coupled PNF.

Taken together, we here describe the generation and functional characterization of ATTO 495- and 647N-labeled EF-C PNF. These covalently labeled fibrils provide many superior features compared to fibrils stained with classical amyloid probes because of their increased brightness, higher stability, and greater sensitivity. Application of these fluorescent fibrils will now foster studies to determine kinetics and dynamics of the interaction of fibrils with cells and viruses along with cellular uptake and transport. Of note, the available ATTO labels enable analysis of the fibrils not only by fluorescence spectroscopy, confocal microscopy, and flow cytometry, as shown herein, but also by time-resolved spectroscopy, fluorescence resonance energy transfer (FRET), single-molecule detection (SMD), and high-resolution fluorescence microscopy as stimulated emission depletion (STED) microscopy and stochastic optical reconstruction microscopy (STORM). Finally, because PNF have prospects to maximize in vivo transduction efficiencies of lentiviral vectors used in gene therapy approaches,[13,24] the covalently labeled PNF presented herein represent ideal tools to study plasma stability and biodistribution in vivo.

EXPERIMENTAL SECTION

Materials and Instruments. Peptides were chemically synthesized and purified by high-performance liquid chroma-

DOI: 10.1021/acs.bioconjchem.7b00079
Bioconjugate Chem. 2017, 28, 1260−1270

tography (HPLC) with a purity of >95% by Synpeptide Co., Ltd. (Shanghai, China). EF-C has the sequence QCKIKQIINMWQ. ATTO 647N and ATTO 495 NHS ester were purchased from ATTO-TEC GmbH (Siegen, Germany, order no. ATTO 647N NHS ester: AD 647N-31 and ATTO 495 NHS ester: AD 495-31). Fluorescence spectroscopy measurements were conducted using Tecan Infinite M1000 PRO plate reader (Männedorf, Zürich, Switzerland) using a 384 well plate with black bottom from Greiner Bio-One (Kremsmünster, Austria). Transmission electron microscopy (Jeol JEM-1400, Akishima, Tokyo, Japan) was used to determine morphology and size of the amyloid fibrils. Confocal microscopy (Zeiss LSM-710, Oberkochen, Germany) was used to detect fluorescence of the fibrils and in cell culture. To determine the amount of fibril-positive cells, we used flow cytometry (BD Canto II, Heidelberg, Germany).

Labeling of EF-C with ATTO 647N and ATTO 495 NHS Ester. The EF-C peptide was lyophilized after synthesis and further diluted in 99.99% DMSO to a final concentration of 10 mg/mL. Labeling was performed according to the manufacturer's protocol using a 2-fold molar excess of the dye. Therefore, we mixed the respective peptide DMSO solution with to 1 mg ATTO NHS dye. The labeling reaction was performed for 1 h at room temperature.

Generation of Labeled ATTO 647N and ATTO 495 PNF. To generate labeled fibrils, ATTO 647N- and ATTO 495-labeled EF-C peptides from the labeling reaction were mixed with unlabeled and untreated peptide at different ratios in 99.99% DMSO. The fibrillation process was initiated by diluting the peptide mixture 10-fold in PBS. Fibrils were formed immediately as described previously.[13] All fibrils were washed three times by centrifugation at 20817*g* for 15 min and resuspended in an equal amount of PBS.

Transmission Electron Microscopy Analysis. Aliquots were removed from the reactions and incubated on glow-discharged (20 mA for 40 s) Formvar carbon coated copper grids (Plano, Wetzlar, Germany) for 5 min at room temperature. The grids were washed three times with double-distilled water before they were counter-stained three times with 2% (w/v) uranyl acetate. The samples were analyzed using a JEM-1400 electron microscope (Jeol, Akishima, Japan) equipped with a TemCam-F216 (TVIPS, Gauting, Germany) at a size of 2048 × 2048 pixels.

Absorption and Fluorescence Spectroscopy. Absorption and fluorescence spectra were recorded on Greiner Bio-one 384 well black plates (Kremsmünster, Austria) and the Tecan Infinite M1000 PRO plate reader (Zürich, Switzerland). All measurements were performed using a 100 μg/mL fibril solution in 1× PBS. For fluorescence emission spectra measurements, 465 and 547 nm were used as excitation wavelengths for ATTO 495 and ATTO 647N, respectively. For single excitation and emission measurements, the following settings were used for ATTO 495, ATTO 647N, p-FTAA, ProteoStat, and ThT, respectively: 498/526, 644/669, 450/510, 550/610, and 450/482 nm. For stability measurements over time, the plate was incubated at 37 °C, and fluorescence was measured every 5 min after 2 s of linear shaking with a 2 mm linear amplitude.

ζ Potential. The surface charge of newly generated fibrils was measured by ζ potential as previously described.[13] Briefly, 50 μL of 1 mg/mL solution was diluted with 950 μL of 1 mM sterile KCl solution. The mixture was measured in a DTS1061 capillary cells (Malvern, Herrenberg, Germany) using the Zeta Nanosizer and the DLS Nano software (Malvern, Herrenberg, Germany). A total of three measurements per sample were performed.

Cell Culture. Adherent TZM-bl reporter cells (NIH Aids Reagent) containing lacZ reporter genes under the control of the HIV long terminal repeat (LTR) promotor and HEK 293T cells (ATCC, CRL-11268) were cultured as described.[13,16] DMEM was used with 120 μg/mL penicillin, 120 μg/mL streptomycin, 350 μg/mL glutamine, and 10% inactivated fetal calf serum (FCS) unless noted otherwise (GIBCO, Carlsbad, CA).

Generation of Retroviral Particles. Virus stocks of HIV-1 NL4-3 92TH014 were generated by transient transfection of 293T cells as described.[40] After transfection and overnight incubation, the transfection mixture was replaced with 2 mL of cell culture medium containing 2.5% inactivated FCS. After 40 h, the culture supernatant was collected and centrifuged for 3 min at 330*g* to remove cell debris. Virus stocks were analyzed by p24 antigen ELISA and stored at −80 °C.

Effect of PNF on Retroviral Infection. The reporter cell line TZM-bl was obtained through the NIH ARRRP and cultured in cell culture medium (DMEM medium supplemented with 120 μg/mL penicillin, 120 μg/mL streptomycin, 350 μg/mL glutamine, and 10% inactivated FCS). This cell line is stably transfected with an LTR-lacZ cassette and expresses CD4, CXCR4, and CCR5. Upon infection with the retrovirus HIV-1, the viral protein Tat is expressed, which activates the LTR resulting in the generation of β-galactosidase. To assess the PNF-mediated enhancement of HIV-1 infection, 10^4 TZM-bl cells in 180 μL of cell culture medium were seeded in 96 well flat-bottom plates (Sarstedt, Nümbrecht, Germany) the day before infection. PNF were preincubated with diluted HIV-1 virus containing ∼0.1 ng p24 antigen. After 10 min, 20 μL of these mixtures were added to TZM-bl cells, and transduction rates were determined 3 days post-infection by measuring β-galactosidase activities in cellular lysates using the Tropix Gal-Screen kit (Applied Biosystems, Life Technologies, Frederick, MD) and the Orion microplate luminometer (Berthold, Bad Wildbad, Germany). All values represent reporter gene activities (RLU/s) derived from triplicate infections minus background activities derived from uninfected cells.

Cell Viability Assay. Possible effects of EF-C PNF were analyzed using TZM-bl cells under the same conditions as described above but in the absence of virus. After 3 days of incubation, intracellular ATP levels were quantified by CellTiter-Glo luminescent cell viability assay (Promega, Fitchburg, WI) as described by the manufacturer. Luminescence signals were measured using an Orion microplate luminometer (Berthold, Bad Wildbad, Germany).

Confocal Microscopy. Fibrils were stained with ThT (Sigma-Aldrich Chemie GmbH, Steinheim, Germany), ProteoStat (Enzo Life Sciences, Farmingdale, NY), and p-FTAA[33] according to the referenced protocols.[31,33,41] For microscopy, TZM-bl cells were seeded in μ-slides (8 well; Ibidi, Munich, Germany) 1 day prior to fibril incubation. Labeled fibrils were incubated with cells at a final concentration of 5 μg/mL in media for 4 h. Cells were then fixed with 4% PFA in 1× PBS. Fibril-only samples were imaged using the same settings with a concentration of 100 μg/mL in μ-slides (18 well; Ibidi, Munich, Germany). All samples were imaged using the Zeiss LSM710 confocal microscope. Excitation wavelengths for ATTO 495, ATTO 647N, p-FTAA, ProteoStat, and ThT were 488, 633, 488, 514, and 405 nm, respectively.

DOI: 10.1021/acs.bioconjchem.7b00079
Bioconjugate Chem. 2017, 28, 1260−1270

Flow Cytometry. For flow cytometry, TZM-bl cells were seeded in 6 well plates (Sarstedt, Nümbrecht, Germany) 1 day prior to incubation with 5 μg/mL of different labeled fibrils for 4 h (day 0), or 3, 6, and 10 days. Thereafter, cells were trypsinized, washed twice with PBS, and fixed with 2% PFA. Cells were analyzed using a BD Canto II (Heidelberg, Germany) and then gated for singlets. Excitation wavelengths for ATTO 647N, ProteoStat, p-FTAA, and ThT were 640, 488, 488, and 405 nm, respectively.

AUTHOR INFORMATION

Corresponding Author

*E-mail: jan.muench@uni-ulm.de.

ORCID

Tanja Weil: 0000-0002-5906-7205

Jan Münch: 0000-0001-7316-7141

Author Contributions

S.R. and M.H. performed most experiments. A.R. helped with flow cytometry. M.L. and S.S. did MALDI-MS. D.M., P.W., and M.F. did electron microscopy. C. M. designed experiments. F.K., T.W., and J.M. supervised work. The manuscript was written through contributions of all authors. All authors have given approval to the final version of the manuscript.

Notes

The authors declare no competing financial interest.

ACKNOWLEDGMENTS

S.R. is funded through a fellowship and is part of the International Graduate School in Molecular Medicine Ulm. A.R. is funded by a fellowship of the Landesgraduiertenförderung Baden-Württemberg and is part of the International Graduate School in Molecular Medicine Ulm. Financial support was provided by grants from the Volkswagen Stiftung (ID: 86366) to F.K., T.W, and J.M. C.M. and S.S. received funding from the Carl Zeiss Stiftung. M.F. and J.M. were also supported by grants from the DFG (FA 456/10 and MU 3115/2-1)

ABBREVIATIONS

EF-C, enhancing factor C; PNF, peptide nanofibril; NHS, *N*-hydroxysuccinimide; MFI, mean fluorescence intensity; RLU, relative light units; RFU, relative fluorescence units; ThT, thioflavin T; TEM, transmission electron microscopy; S-to-N, signal-to-noise

REFERENCES

(1) Andreadis, S., Lavery, T., Davis, H. E., Le Doux, J. M., Yarmush, M. L., and Morgan, J. R. (2000) Toward a more accurate quantitation of the activity of recombinant retroviruses: alternatives to titer and multiplicity of infection. *J. Virol. 74*, 3431−3439.

(2) Nayerossadat, N., Maedeh, T., and Ali, P. A. (2012) Viral and nonviral delivery systems for gene delivery. *Adv. Biomed. Res. 1*, 27.

(3) Chuck, A. S., Clarke, M. F., and Palsson, B. O. (1996) Retroviral infection is limited by Brownian motion. *Hum. Gene Ther. 7*, 1527−1534.

(4) Le Doux, J. M., Davis, H. E., Morgan, J. R., and Yarmush, M. L. (1999) Kinetics of retrovirus production and decay. *Biotechnol. Bioeng. 63*, 654−662.

(5) Hodgson, C. P., and Solaiman, F. (1996) Virosomes: cationic liposomes enhance retroviral transduction. *Nat. Biotechnol. 14*, 339−342.

(6) Vogt, P. K. (1967) DEAE-dextran: enhancement of cellular transformation induced by avian sarcoma viruses. *Virology 33*, 175−177.

(7) Lin, P., Correa, D., Lin, Y., and Caplan, A. I. (2011) Polybrene inhibits human mesenchymal stem cell proliferation during lentiviral transduction. *PLoS One 6*, e23891.

(8) Davis, H. E., Rosinski, M., Morgan, J. R., and Yarmush, M. L. (2004) Charged polymers modulate retrovirus transduction via membrane charge neutralization and virus aggregation. *Biophys. J. 86*, 1234−1242.

(9) Cornetta, K., and Anderson, W. F. (1989) Protamine sulfate as an effective alternative to Polybrene in retroviral-mediated gene-transfer: implications for human gene therapy. *J. Virol. Methods 23*, 187−194.

(10) Toyoshima, K., and Vogt, P. K. (1969) Enhancement and inhibition of avian sarcoma viruses by polycations and polyanions. *Virology 38*, 414−426.

(11) Davis, H. E., Morgan, J. R., and Yarmush, M. L. (2002) Polybrene increases retrovirus gene transfer efficiency by enhancing receptor-independent virus adsorption on target cell membranes. *Biophys. Chem. 97*, 159−172.

(12) Meier, C., Weil, T., Kirchhoff, F., and Münch, J. (2014) Peptide nanofibrils as enhancers of retroviral gene transfer. *Wiley Interdiscip Rev. Nanomed Nanobiotechnol 6*, 438−451.

(13) Yolamanova, M., Meier, C., Shaytan, A. K., Vas, V., Bertoncini, C. W., Arnold, F., Zirafi, O., Usmani, S. M., Müller, J. A., Sauter, D., Goffinet, C., Palesch, D., Walther, P., Roan, N. R., Geiger, H., Lunov, O., Simmet, T., Bohne, J., Schrezenmeier, H., Schwarz, K., Ständker, L., Forssmann, W.-G., Salvatella, X., Khalatur, P. G., Khokhlov, A. R., Knowles, T. P. J., Weil, T., Kirchhoff, F., and Münch, J. (2013) Peptide nanofibrils boost retroviral gene transfer and provide a rapid means for concentrating viruses. *Nat. Nanotechnol. 8*, 130−136.

(14) Zhang, L., Jiang, C., Zhang, H., Gong, X., Yang, L., Miao, L., Shi, Y., Zhang, Y., Kong, W., Zhang, C., and Shan, Y. (2014) A novel modified peptide derived from membrane-proximal external region of human immunodeficiency virus type 1 envelope significantly enhances retrovirus infection. *J. Pept. Sci. 20*, 46−54.

(15) Zhang, H., He, X., Shi, Y., Yu, Y., Guan, S., Gong, X., Yin, H., Kuai, Z., and Shan, Y. (2016) Potential of a novel peptide P16-D from the membrane-proximal external region of human immunodeficiency virus type 1 to enhance retrovirus infection. *RSC Adv. 6*, 82082−82087.

(16) Münch, J., Rücker, E., Adermann, K., Schindler, M., Wildum, S., Chinnadurai, R., Rajan, D., Specht, A., Giménez-Gallego, G., Sánchez, P. C., Fowler, D. M., Koulov, A., Kelly, J. W., Mothes, W., Grivel, J.-C., Margolis, L., Keppler, O. T., Forssmann, W.-G., Kirchhoff, F., Ständker, L., and Goffinet, C. (2007) Semen-derived amyloid fibrils drastically enhance HIV infection. *Cell 131*, 1059−1071.

(17) Wurm, M., Schambach, A., Lindemann, D., Hanenberg, H., Ständker, L., Forssmann, W.-G., Blasczyk, R., and Horn, P. A. (2010) The influence of semen-derived enhancer of virus infection on the efficiency of retroviral gene transfer. *J. Gene Med. 12*, 137−146.

(18) Fändrich, M. (2007) On the structural definition of amyloid fibril and other polypeptide aggregates. *Cell. Mol. Life Sci. 64*, 2066−2078.

(19) Rambaran, R., and Serpell, L. (2008) Amyloid fibrils: abnormal protein assembly. *Prion 2*, 112−117.

(20) Roan, N. R., Münch, J., Arhel, N., Mothes, W., Neidleman, J., Kobayashi, A., Smith-McCune, K., Kirchhoff, F., and Greene, W. C. (2009) The cationic properties of SEVI underlie its ability to enhance human immunodeficiency virus infection. *J. Virol. 83*, 73−80.

(21) Roan, N. R., Sowinski, S., Münch, J., Kirchhoff, F., and Greene, W. C. (2010) Aminoquinoline surfen inhibits the action of SEVI (semen-derived enhancer of viral infection). *J. Biol. Chem. 285*, 1861−1869.

(22) Arnold, F., Schnell, J., Zirafi, O., Stürzel, C., Meier, C., Weil, T., Ständker, L., Forssmann, W.-G., Roan, N. R., Greene, W. C., Kirchhoff, F., and Münch, J. (2012) Naturally occurring fragments from two distinct regions of the prostatic acid phosphatase form amyloidogenic enhancers of HIV infection. *J. Virol. 86*, 1244−1249.

(23) Roan, N. R., Müller, J. A., Liu, H., Chu, S., Stürzel, C. M., Walther, P., Dong, M., Witkowska, H. E., Kirchhoff, F., Münch, J., Greene, W. C., and Arnold, F. (2011) Peptides released by

DOI: 10.1021/acs.bioconjchem.7b00079
Bioconjugate Chem. 2017, 28, 1260−1270

physiological cleavage of semen coagulum proteins form amyloids that enhance HIV infection. *Cell Host Microbe 10*, 541−550.
(24) Cai, Y., Laustsen, A., Zhou, Y., Sun, C., Anderson, M. V., Li, S., Uldbjerg, N., Luo, Y., Jakobsen, M. R., and Mikkelsen, J. G. (2016) Targeted, homology-driven gene insertion in stem cells by ZFN-loaded "all-in-one" lentiviral vectors. *eLife 5*, 458.
(25) Westermark, G. T., Johnson, K. H., and Westermark, P. (1999) Staining methods for identification of amyloid in tissue. *Methods Enzymol. 309*, 3−25.
(26) Howie, A. J., Brewer, D. B., Howell, D., and Jones, A. P. (2008) Physical basis of colors seen in Congo red-stained amyloid in polarized light. *Lab. Invest. 88*, 232−242.
(27) Fernandez-Flores, A. (2011) A review of amyloid staining: methods and artifacts. *Biotech. Histochem. 86*, 293−301.
(28) Biancalana, M., and Koide, S. (2010) Molecular mechanism of Thioflavin-T binding to amyloid fibrils. *Biochim. Biophys. Acta, Proteins Proteomics 1804*, 1405−1412.
(29) Amdursky, N., Erez, Y., and Huppert, D. (2012) Molecular Rotors: What Lies Behind the High Sensitivity of the Thioflavin-T Fluorescent Marker. *Acc. Chem. Res. 45*, 1548−1557.
(30) Bolder, S. G., Sagis, L. M. C., Venema, P. A., and van der Linden, E. (2007) Thioflavin T and Birefringence Assays to Determine the Conversion of Proteins into Fibrils. *Langmuir 23*, 4144−4147.
(31) Shen, D., Coleman, J., Chan, E., Nicholson, T. P., Dai, L., Sheppard, P. W., and Patton, W. F. (2011) Novel cell- and tissue-based assays for detecting misfolded and aggregated protein accumulation within aggresomes and inclusion bodies. *Cell Biochem. Biophys. 60*, 173−185.
(32) Freire, S., de Araujo, M. H., Al-Soufi, W., and Novo, M. (2014) Photophysical study of Thioflavin T as fluorescence marker of amyloid fibrils. *Dyes Pigm. 110*, 97−105.
(33) Aslund, A., Sigurdson, C. J., Klingstedt, T., Grathwohl, S., Bolmont, T., Dickstein, D. L., Glimsdal, E., Prokop, S., Lindgren, M., Konradsson, P., Holtzman, D. M., Hof, P. R., Heppner, F. L., Gandy, S., Jucker, M., Aguzzi, A., Hammarström, P., and Nilsson, K. P. R. (2009) Novel Pentameric Thiophene Derivatives for in Vitroand in VivoOptical Imaging of a Plethora of Protein Aggregates in Cerebral Amyloidoses. *ACS Chem. Biol. 4*, 673−684.
(34) Usmani, S. M., Zirafi, O., Müller, J. A., Sandi-Monroy, N. L., Yadav, J. K., Roan, N. R., Greene, W. C., Nilsson, K. P. R., Hammarström, P., Wetzel, R., Pilcher, C. D., Gagsteiger, F., Faendrich, M., Kirchhoff, F., Münch, J., Meier, C., Weil, T., and Walther, P. (2014) Direct visualization of HIV-enhancing endogenous amyloid fibrils in human semen. *Nat. Commun. 5*, 3508.
(35) Viegas, M. S., Martins, T. C., Seco, F., and do Carmo, A. (2007) An improved and cost-effective methodology for the reduction of autofluorescence in direct immunofluorescence studies on formalin-fixed paraffin-embedded tissues. *Eur. J. Histochem 51*, 59−66.
(36) Hudson, S. A., Ecroyd, H., Kee, T. W., and Carver, J. A. (2009) The thioflavin T fluorescence assay for amyloid fibril detection can be biased by the presence of exogenous compounds. *FEBS J. 276*, 5960−5972.
(37) Sulatskaya, A. I., Kuznetsova, I. M., and Turoverov, K. K. (2011) Interaction of thioflavin T with amyloid fibrils: stoichiometry and affinity of dye binding, absorption spectra of bound dye. *J. Phys. Chem. B 115*, 11519−11524.
(38) Groenning, M. (2010) Binding mode of Thioflavin T and other molecular probes in the context of amyloid fibrils-current status. *J. Chem. Biol. 3*, 1−18.
(39) Chen, S., Berthelier, V., Hamilton, J. B., O'Nuallai, B., and Wetzel, R. (2002) Amyloid-like features of polyglutamine aggregates and their assembly kinetics. *Biochemistry 41*, 7391−7399.
(40) Münch, J., Adermann, K., Schulz, A., Schindler, M., Chinnadurai, R., Pöhlmann, S., Chaipan, C., Biet, T., Peters, T., Meyer, B., Wilhelm, D., Lu, H., Jing, W., Jiang, S., Forssmann, W.-G., Kirchhoff, F., and Ständker, L. (2007) Discovery and Optimization of a Natural HIV-1 Entry Inhibitor Targeting the gp41 Fusion Peptide. *Cell 129*, 263−275.
(41) Nilsson, M. R. (2004) Techniques to study amyloid fibril formation in vitro. *Methods 34*, 151−160.
(42) Giannotti, M. I., Esteban, O., Oliva, M., García-Parajo, M. F., and Sanz, F. (2011) pH-responsive polysaccharide-based polyelectrolyte complexes as nanocarriers for lysosomal delivery of therapeutic proteins. *Biomacromolecules 12*, 2524−2533.
(43) Zhegalova, N. G., He, S., Zhou, H., Kim, D. M., and Berezin, M. Y. (2014) Minimization of self-quenching fluorescence on dyes conjugated to biomolecules with multiple labeling sites via asymmetrically charged NIR fluorophores. *Contrast Media Mol. Imaging 9*, 355−362.
(44) Swiecicki, J.-M., Thiebaut, F., Di Pisa, M., Gourdin-Bertin, S., Tailhades, J., Mansuy, C., Burlina, F., Chwetzoff, S., Trugnan, G., Chassaing, G., and Lavielle, S. (2016) How to unveil self-quenched fluorophores and subsequently map the subcellular distribution of exogenous peptides. *Sci. Rep. 6*, 20237.
(45) Lakowicz, J. R. (2007) *Principles of Fluorescence Spectroscopy* (Lakowicz, J. R., Ed.), Springer Science & Business Media, Boston, MA.
(46) Charneau, P., Mirambeau, G., Roux, P., Paulous, S., Buc, H., and Clavel, F. (1994) HIV-1 reverse transcription. A termination step at the center of the genome. *J. Mol. Biol. 241*, 651−662.
(47) Mädler, S., Bich, C., Touboul, D., and Zenobi, R. (2009) Chemical cross-linking with NHS esters: a systematic study on amino acid reactivities. *J. Mass Spectrom. 44*, 694−706.
(48) Roberti, M. J., Fölling, J., Celej, M. S., Bossi, M., Jovin, T. M., and Jares-Erijman, E. A. (2012) Imaging nanometer-sized α-synuclein aggregates by superresolution fluorescence localization microscopy. *Biophys. J. 102*, 1598−1607.
(49) Ruiz, J., Boehringer, R., Grogg, M., Raya, J., Schirer, A., Crucifix, C., Hellwig, P., Schultz, P., and Torbeev, V. (2016) Covalent Tethering and Residues with Bulky Hydrophobic Side Chains Enable Self-Assembly of Distinct Amyloid Structures. *ChemBioChem 17*, 2274−2285.
(50) Gerling, U. I. M., Salwiczek, M., Cadicamo, C. D., Erdbrink, H., Czekelius, C., Grage, S. L., Wadhwani, P., Ulrich, A. S., Behrends, M., Haufe, G., and Koksch, B. (2014) Fluorinated amino acids in amyloid formation: a symphony of size, hydrophobicity and α-helix propensity. *Chemical Science 5*, 819−830.
(51) Swiecicki, J.-M., Thiebaut, F., Di Pisa, M., Gourdin-Bertin, S., Tailhades, J., Mansuy, C., Burlina, F., Chwetzoff, S., Trugnan, G., Chassaing, G., and Lavielle, S. (2016) How to unveil self-quenched fluorophores and subsequently map the subcellular distribution of exogenous peptides. *Sci. Rep. 6*, 20237.
(52) Doyle, A. D., Carvajal, N., Jin, A., Matsumoto, K., and Yamada, K. M. (2015) Local 3D matrix microenvironment regulates cell migration through spatiotemporal dynamics of contractility-dependent adhesions. *Nat. Commun. 6*, 8720.
(53) Hussein, R. M., Hashem, R. M., and Rashed, L. A. (2015) Evaluation of the amyloid beta-GFP fusion protein as a model of amyloid beta peptides-mediated aggregation: a study of DNAJB6 chaperone. *Front. Mol. Neurosci. 8*, 40.
(54) Rey, N. L., Petit, G. H., Bousset, L., Melki, R., and Brundin, P. (2013) Transfer of human α-synuclein from the olfactory bulb to interconnected brain regions in mice. *Acta Neuropathol. 126*, 555−573.
(55) Brahic, M., Bousset, L., Bieri, G., Melki, R., and Gitler, A. D. (2016) Axonal transport and secretion of fibrillar forms of α-synuclein, Aβ42 peptide and HTTExon 1. *Acta Neuropathol. 131*, 539−548.
(56) Freundt, E. C., Maynard, N., Clancy, E. K., Roy, S., Bousset, L., Sourigues, Y., Covert, M., Melki, R., Kirkegaard, K., and Brahic, M. (2012) Neuron-to-neuron transmission of α-synuclein fibrils through axonal transport. *Ann. Neurol. 72*, 517−524.
(57) Bousset, L., Brundin, P., Böckmann, A., Meier, B., and Melki, R. (2016) An Efficient Procedure for Removal and Inactivation of Alpha-Synuclein Assemblies from Laboratory Materials. *J. Parkinson's Dis. 6*, 143−151.
(58) Apetri, M. M., Harkes, R., Subramaniam, V., Canters, G. W., Schmidt, T., and Aartsma, T. J. (2016) Direct Observation of α-Synuclein Amyloid Aggregates in Endocytic Vesicles of Neuroblastoma Cells. *PLoS ONE 11*, e0153020.

DOI: 10.1021/acs.bioconjchem.7b00079
Bioconjugate Chem. 2017, 28, 1260−1270

(59) Brown, J. W. P., Buell, A. K., Michaels, T. C. T., Meisl, G., Carozza, J., Flagmeier, P., Vendruscolo, M., Knowles, T. P. J., Dobson, C. M., and Galvagnion, C. (2016) β-Synuclein suppresses both the initiation and amplification steps of α-synuclein aggregation via competitive binding to surfaces. *Sci. Rep. 6*, 36010.
(60) McWilliams-Koeppen, H. P., Foster, J. S., Hackenbrack, N., Ramirez-Alvarado, M., Donohoe, D., Williams, A., Macy, S., Wooliver, C., Wortham, D., Morrell-Falvey, J., Foster, C. M., Kennel, S. J., and Wall, J. S. (2015) Light Chain Amyloid Fibrils Cause Metabolic Dysfunction in Human Cardiomyocytes. *PLoS ONE 10*, e0137716.
(61) Jin, S., Kedia, N., Illes-Toth, E., Haralampiev, I., Prisner, S., Herrmann, A., Wanker, E. E., and Bieschke, J. (2016) Amyloid-β(1−42) Aggregation Initiates Its Cellular Uptake and Cytotoxicity. *J. Biol. Chem. 291*, 19590−19606.

DOI: 10.1021/acs.bioconjchem.7b00079
Bioconjugate Chem. 2017, 28, 1260−1270